Image Anal Stereol 2023;42:145-159 doi: 105566/ias.2824
Original Research Paper

A COMPLETED MULTIPLE THRESHOLD ENCODING PATTERN FOR TEXTURE CLASSIFICATION

BIN LI[1], YIBING LI ✉,[1], Q.M. JONATHAN WU[2]

[1]Harbin Engineering University, the Key Laboratory of Advanced Marine Communication and Information Technology, Ministry of Industry and Information Technology, Department of Information and Communication Engineering, Street Nantong, Harbin, China, 150001;[2]University of Windsor, 401 Sunset Avenue, Windsor, Canada, N9B3P4

e-mail: libin_heu@hrbeu.edu.cn; liyibing0920@126.com; jwu@uwindsor.ca

(Received November 6, 2022; revised July 2, 2023; accepted July 9, 2023)

ABSTRACT

The binary pattern family has drawn wide attention for texture representation due to its promising performance and simple operation. However, most binary pattern methods focus on local neighborhoods but ignore center pixels. Even if some studies introduce the center based sub-pattern to provide complementary information, existing center based sub-patterns are much weaker than other local neighborhood based sub-patterns. This severe unbalance limits the classification performance of fusion features significantly. To alleviate this problem, this paper designs a multiple threshold center pattern (MTCP) to provide a more discriminative and complementary local texture representation with a compact form. First, a multiple threshold encoding strategy is designed to encode the center pixel that generates three 1-bit binary patterns. Second, it adopts a compact multi-pattern encoding strategy to combine them into a 3-bit MTCP. Furthermore, this paper proposes a completed multiple threshold encoding pattern by fusing the MTCP, local sign pattern, and local magnitude pattern. Comprehensive experimental evaluations on three popular texture classification benchmarks confirm that the completed multiple threshold encoding pattern achieves superior texture classification performance.

Keywords: binary pattern, completed encoding, image texture analysis, texture image classification.

INTRODUCTION

Texture classification is a promising sub-field in image processing and pattern recognition. It has attracted much attention because of its wide range of practical applications, including face recognition (Tan and Triggs, 2010; Chakraborty *et al.*, 2017a; 2018; 3. Taha *et al.*, 2020), scene detection (Wei and Dai, 2016), palmprint recognition (Fei *et al.*, 2020), medical image analysis (Nie *et al.*, 2021), and video processing (Lee *et al.*, 2015; Dimitropoulos *et al.*, 2017). However, it is still a challenging task to develop an efficient and discriminative texture descriptor under complex imaging conditions, such as illumination and rotation variation, viewpoint, and scale changes.

In the past two decades, the binary pattern family has shown promising results (Ojala *et al.*, 2002; Guo *et al.*, 2010; Zhang *et al.*, 2017; Sotoodeh *et al.*, 2019; Pan *et al.*, 2020; Li *et al.*, 2018; Nanni *et al.*, 2010; Armi and Fekri-Ershad, 2019; Murala *et al.*, 2012; Wang *et al.*, 2015; Chakraborty *et al.*, 2017b; Song *et al.*, 2018; Song *et al.*, 2015; Pan *et al.*, 2017; Xu *et al.*, 2020a; 2021) in addressing problematic challenges of texture analysis due to its computation efficiency and discriminative power. In this paradigm, local neighborhood pixels are firstly quantified by a threshold that is defined as the center pixel value in most cases. For example, the local binary pattern (LBP) (Ojala *et al.*, 2002) used the center pixel as the encoding threshold to generate the binary pattern. Then, based on the binary coding, a decimal code number is generated to represent the local neighborhood structure. Finally, the frequency histogram of the code number is used as the feature vector to classify the texture image.

To further improve the classification performance, many researchers introduce complementary texture information to enhance the texture descriptor. The most famous method is the completing modeling of LBP (CLBP) (Guo *et al.*, 2010), that consists of the sign, magnitude, and center components. The center and magnitude components provide useful complementary information to the sign component, which improves the texture classification performance significantly. Zhang *et al.* (2017) proposed the completed discriminative local

features (CDLF) that not only inherits the advantages of CLBP, but also learn a transformation matrix and use an adaptive weight strategy to enhance the classification performance. Sotoodeh *et al.* (2019) followed the framework of CLBP and developed a color radial mean CLBP for color image retrieval. Pan *et al.* (2020) designed a scale-adaptive LBP (SALBP) based on CLBP that adaptively find a single and optimal scale for binary encoding to address scale variations. Li *et al.* (2018) designed a circular regional mean operation to enhance the robustness of CLBP. Based on the above analysis, we find that the center based sub-pattern is much weaker than other local neighborhood based sub-patterns. This unbalance is a serious inherent drawback that significantly limits the texture classification accuracy.

The most effective way to alleviate the unbalance is to design a more discriminative center based sub-pattern. Unfortunately, no researcher studied how to provide a more powerful representation of the center based sub-pattern. To solve this problem, we research many methods for enhancing binary patterns and find that the encoding threshold strategy plays a crucial role in related processes. More specifically, the local ternary pattern (LTP) (Tan and Triggs, 2010) introduced a 3-value encoding strategy to encode local differences and generate ternary patterns, which showed a superior performance for face recognition. Similarly, Nanni *et al.* (2010) proposed the local quinary pattern (LQP), which used two thresholds to split the local neighborhood into four binary codes. Based on LQP, Armi and Fekri-Ershad (2019) proposed a dynamic threshold strategy to enhance the dividing process of quinary patterns and developed the improved LQP (ILQP). Other similar methods include local tetra pattern (LTrP) (Murala *et al.*, 2012), local N-ary pattern (LNP) (Wang *et al.*, 2015), and local quadruple pattern (LQPAT) (Chakraborty *et al.*, 2017b). The above analysis shows that different types of threshold strategies can be of great help to extract additional discriminant information. Moreover, for exploiting more comprehensive texture information, Song *et al.* (2018) developed the locally encoded transform feature histogram which adopts binary and multi-thresholding to implement scalar quantization. Song *et al.* (2015) designed a powerful threshold strategy by an adjacent evaluation window and proposed the adjacent evaluation local binary pattern. Pan *et al.* (2017) presented an adaptive local threshold scheme to encode the local mean and variance component and proposed the feature based local binary pattern (FbLBP). Recently, Xu *et al.* (2020a) developed a multi-scale hierarchical threshold for visual texture classification, which helped the texture descriptor to extract both micro- and macro-structure features. In Xu *et al.* (2021), based on the multi-scale hierarchical threshold, a compact encoding strategy was proposed to combine three 1-bit sub-patterns into a 3-bit binary pattern. By this way, it not only provides a highly compact feature representation, but also achieves a satisfactory classification performance.

Although binary pattern methods have achieved great successes, there are still some problems to be solved. First, most of thresholding schemes usually focus on extracting local neighborhood differences but ignore other local components, such as center pixels. Second, center based sub-patterns are much weaker than other local neighborhood based sub-patterns. Third, how to effectively integrate binary patterns extracted by different thresholds is a crucial issue for feature representation. In order to solve these issues, this paper introduces a new multiple threshold encoding strategy for encoding the center pixel and proposes a completed multiple threshold encoding pattern for texture classification task. The contributions of this paper are as follows:

1. This paper designs a novel multiple threshold encoding strategy that introduces three sub-thresholds to encode the center pixel into three 1-bit binary patterns at the same time.
2. A multi-threshold center pattern (MTCP) is proposed by encoding the three 1-bit binary sub-patterns into a 3-bit binary pattern with a compact multi-pattern encoding strategy.
3. This paper develops a completed multiple threshold encoding pattern (CMTEP) by jointly fusing the MTCP, local sign pattern, and local magnitude pattern.
4. Extensive experimental evaluations on three popular texture classification benchmarks demonstrate that the CMTEP offers a powerful texture representation and achieves superior texture classification performances.

MATERIALS AND METHODS

REVIEW OF CLBP

As the base of the proposed texture descriptor, we review the CLBP in this section. The CLBP was first proposed by Guo *et al.* (2010) and has become one of the most successful completed modeling of local neighborhood. In the CLBP, the local texture region is divided into three complementary sub-components: the local center, local signs and local magnitudes. Then, they are encoded into CLBP_C, CLBP_S, and CLBP_M, respectively.

For a center pixel g_c, its corresponding radius R, and neighbors $g_{R,p}$, $p=0,...,P-1$, where P is the number of neighbors, the CLBP_S can be formulated as:

$$CLBP\_S_{R,P}=\sum_{p=0}^{P-1}s\left(g_{R,p}-g_c\right)2^p, \tag{1}$$

where $s(\bullet)$ is the sign function, defined as

$$s(x)=H(x)=\begin{cases}1, x\geq 0\\ 0, x<0\end{cases}. \tag{2}$$

Here, $H(x)$ is the standard Heaviside function. Suppose the coordinates of g_c are (0,0), then the coordinates of the value of $g_{R,p}$ are $(R\cos(2\pi p/P), R\sin(2\pi p/P))$. The gray value of $g_{R,p}$ that is not in the image grids can be estimated by interpolation.

Like most LBP variants, the classical rotation invariant uniform pattern (riu2) is implemented with a lookup table of its histogram, represented as $CLBP\_S_{R,P}^{riu2}$. Suppose the image is of size $I\times J$. After the $CLBP\_S_{R,P}^{riu2}$ pattern of each pixel is encoded, a histogram is built to represent the texture image. In the $CLBP\_S_{R,P}^{riu2}$ histogram, the number of bins is $P+2$, the value of each bin is defined:

$$His(b)=\sum_{i=1}^{I}\sum_{j=1}^{J}f(CLBP\_S_{R,P}^{riu2}(i,j),b), b\in\left[0,(P+2)-1\right], \tag{3}$$

$$f(x,y)=\begin{cases}1, x=y\\ 0, otherwise\end{cases}. \tag{4}$$

The CLBP_M expresses the local difference magnitude information, that is described as:

$$CLBP\_M_{R,P}=\sum_{p=0}^{P-1}t\left(m_{R,p},c_m\right)2^p, \tag{5}$$

where $t(.)$ is the threshold function, described as

$$t(x,c)=H(x-c). \tag{6}$$

Here, $H(.)$ is the standard Heaviside function defined in (2).

In (5), $m_{R,p}=\left|g_{R,p}-g_c\right|$ is the local difference magnitude. c_m is the threshold corresponding to $m_{R,p}$, that is given as the average value of $m_{R,p}$ for the whole image. Like $CLBP\_S_{R,P}^{riu2}$, the rotation invariant uniform version, $CLBP\_M_{R,P}^{riu2}$, is used for feature representation.

As a vital and necessary part of the local texture, the center pixel contains some important information of local pixel gray levels, and the CLBP_C is obtained by

$$CLBP\_C_{R,P}=t\left(g_c,c_I\right), \tag{7}$$

where $t(.)$ is defined in (6). c_I is the threshold that is calculated by the average of the whole image gray level. The center pixel is encoded as a 1-bit binary code by formula (7).

As in Guo *et al.* (2010), the three local sub-patterns can be fused by two ways: jointly and in a hybrid way. Therefore, we can obtain different fused features, such as CLBP_M_S/C, CLBP_S_M/C, and CLBP_S/M/C.

It is worth noting that CLBP_C is much weaker than CLBP_S and CLBP_M due to its 1-bit feature dimension. Although the center pixel can provide very important complementary information for the local texture analysis, the severe unbalance of the sub-pattern representation limits the texture classification performance significantly. So, it is highly promising to design a more powerful feature representation for the center pixel instead of encoding it into a simply 1-bit binary code.

A COMPLETED MULTIPLE THRESHOLD ENCODING PATTERN

Multiple Threshold Center Pattern

For the CLBP, the expressive power of its local center component is much weaker than the other two components as explained below. This severe unbalance significantly limits the classification performance. The reason of this unbalance is that the local center component utilizes a single threshold to generate a 1-bit sub-pattern.

To facilitate the analysis and understanding, we give a 3D analysis in Fig. 1. Fig. 1(a) is the texture image I. Fig. 1(b) shows the texture image and its threshold c_I in the three-dimensional surface plot. Fig. 1(c) is the CLBP_C code obtained by threshold c_I. We can notice that the local texture information obtained by the single threshold c_I is very limited, because it gives a binary image (Fig.1(c)). The rough quantization method fails to offer a discriminative sub-feature that leads to the unbalance between the center based sub-pattern and other local neighborhood based sub-patterns.

The most efficient and feasible method to alleviate this unbalance is to design an appropriate strategy for enhancing the expressive power of the center pattern. Many researchers have developed some strategies for promoting the discriminative power of binary pattern

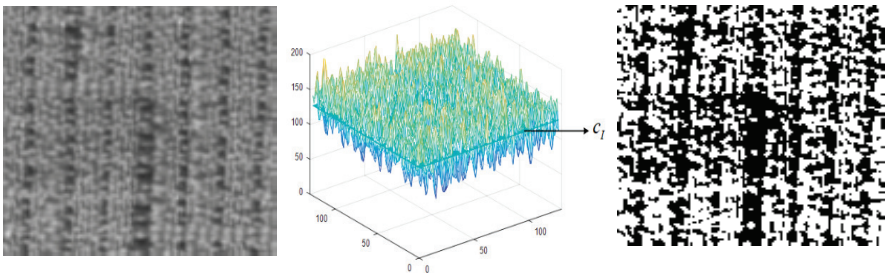

Fig. 1. *The texture image and its CLBP_C code: (a) The texture image, (b) 3D surface plot of the texture image and its threshold* c_I*, (c) The CLBP_C code.*

methods. Instead of the single threshold in LBP, the local ternary pattern (LTP) (Tan and Triggs, 2010) used multi-thresholds and proposed a 3-value encoding scheme to evaluate the local gray-scale difference. After that, the local quinary pattern (LQP) (Nanni *et al.,* 2010) and local N-ary pattern (LNP) (Wang *et al*., 2015) and its extensions were proposed to employ underlying local texture information that significantly enhanced the local texture representation power.

Inspired by this, we design a novel multiple threshold encoding strategy to improve the traditional single threshold encoding strategy. Our new strategy explores highly discriminative information from center pixels. Specifically, it introduces three sub-thresholds to encode the center pixel from different points of view, then it utilizes a compact multi-pattern encoding strategy to combine the three 1-bit binary sub-patterns into a 3-bit pattern, called multiple threshold center pattern (MTCP). By this way, the MTCP offers a more discriminative local texture representation, and at the same time it keeps a satisfying feature simplicity.

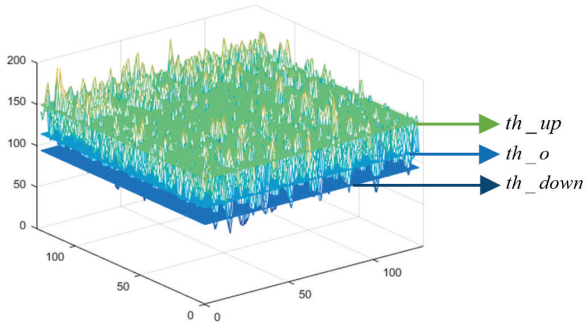

Fig. 2. *Illustration of multiple thresholds.*

Given a texture image I, g_c is the center pixel, and th_o is the hierarchical multi-scale threshold, which is presented in Xu *et al.* (2020a), as shown in Fig. 3:

$$th\_o = thre_{N,g_c} = \frac{1}{N}\sum_{k=1}^{N} lm_k(g_c), \tag{8}$$

where $lm_k(g_c)$ is the local mean of g_c on the grid partitioning with scale k. N is the number of hierarchical scales.

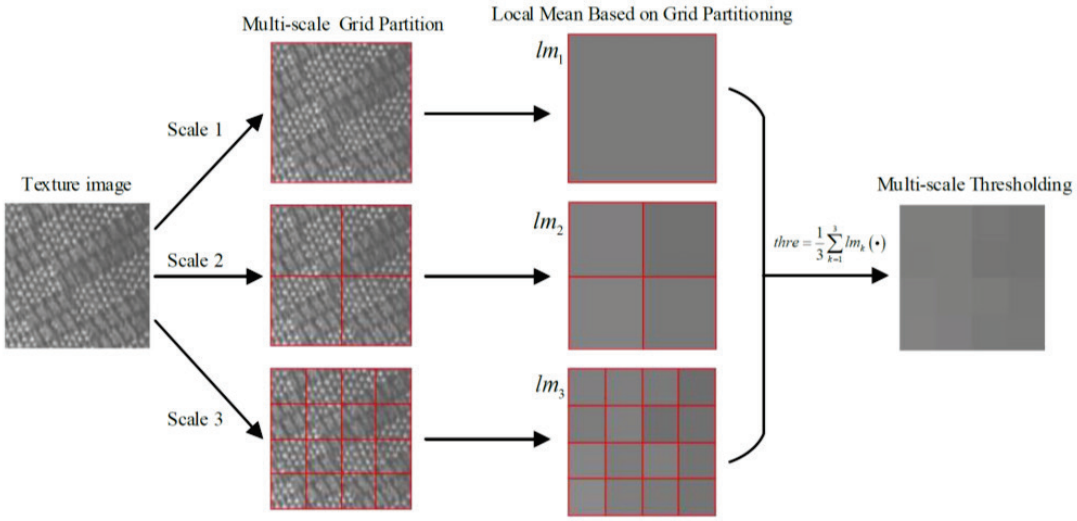

Fig. 3. *Illustration of hierarchical multi-scale thresholds (Xu et al., 2020a).*

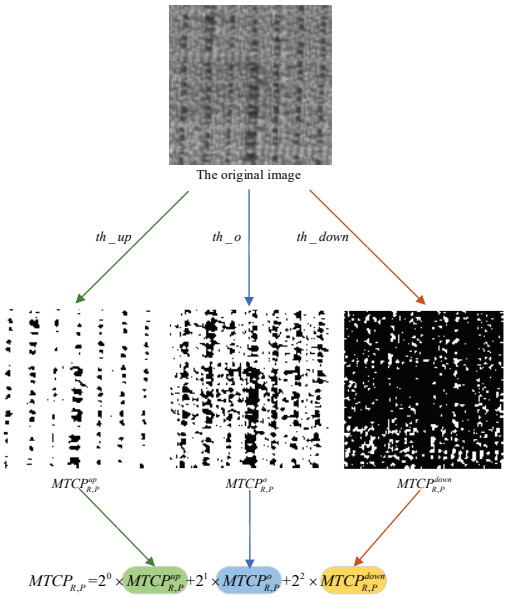

Fig. 4. *The illustration of our MTCP.*

The parameters th_up and th_down are obtained by moving th_o up and down, as shown in Fig. 2. They are represented as:

$$th\_up = \alpha \times th\_o, \tag{9}$$

$$th\_down = \beta \times th\_o, \tag{10}$$

where $\alpha > 1$ and $0 < \beta < 1$ are floating parameters. For α and β, we introduce a controlling factor $\gamma\,(0 < \gamma < 1)$ to adjust them: $\alpha = 1 + \gamma$ and $\beta = 1 - \gamma$.

Then, we can get three 1-bit binary patterns by encoding the center pixel with th_up, th_o, and th_down, which are defined as:

$$MTCP^{up}_{R,P} = t\left(g_c, th\_up\right), \tag{11}$$

$$MTCP^{o}_{R,P} = t\left(g_c, th\_o\right), \tag{12}$$

$$MTCP^{down}_{R,P} = t\left(g_c, th\_down\right). \tag{13}$$

Similar to CLBP_C, $MTCP^{up}_{R,P}$, $MTCP^{o}_{R,P}$, and $MTCP^{down}_{R,P}$ are only 1-bit, that cannot work well independently. So, how to combine them is an important problem to be solved.

To achieve a more compact and efficient feature representation, Xu *et al.* (2021) introduce an MMC pattern, which encodes three 1-bit binary patterns into a 3-bit binary code. For this purpose, this paper utilizes the similar fusion strategy to combine $MTCP^{up}_{R,P}$, $MTCP^{o}_{R,P}$, and $MTCP^{down}_{R,P}$ into a new 3-bit binary code, named multiple threshold center pattern (MTCP). It is defined as:

$$MTCP_{R,P} = 2^0 \times MTCP^{up}_{R,P} + 2^1 \times MTCP^{o}_{R,P} + 2^2 \times MTCP^{down}_{R,P}. \tag{14}$$

Fig. 4 illustrates the process to obtain the MTCP descriptor. For example, if the $MTCP^{up}_{R,P}$ is $(0)_2$ in binary numeral system, the $MTCP^{o}_{R,P}$ is $(1)_2$, and the $MTCP^{down}_{R,P}$ is $(1)_2$, the final MTCP is $(110)_2 = (6)_{10}$ in decimal numeral system. Fig. 5 shows the correlation coefficients between different images binarized by th_up, th_o, and th_down. We select 1000 images from UMD database to compute the correlation co efficients and report their means. C-o-up is the average

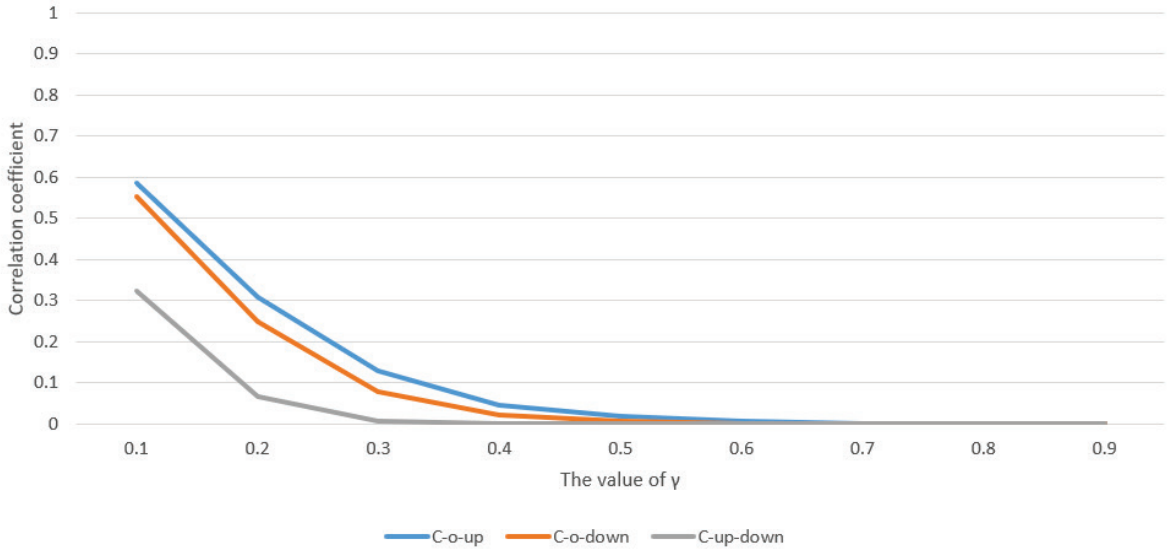

Fig. 5. *The analysis of correlation coefficients.*

correlation coefficients between binarized images with th_o and th_up, C-o-down is the average correlation coefficients between binarized images with th_o and th_down, C-up-down is the average correlation coefficients between binarized images with th_up and th_down. We can easily find that $MTCP^{up}_{R,P}$, $MTCP^{o}_{R,P}$, and $MTCP^{down}_{R,P}$ do not have high correlation. In this paper, we set $\gamma = 0.2$ as shown in Section RESULTS, which provides low correlation. It proves that $MTCP^{up}_{R,P}$, $MTCP^{o}_{R,P}$, and $MTCP^{down}_{R,P}$ offer more rich texture information from the local center component. Compared with the CLBP_C, the MTCP is more informative and discriminative while it keeps a reasonable feature dimension.

A Completed Multiple Threshold Encoding Pattern

To obtain a more comprehensive feature representation, a completed multiple threshold encoding pattern (CMTEP) is developed by jointly fusing the MTCP, local sign pattern, and local magnitude pattern. As shown in Fig. 6, the proposed CMTEP contains three components: $CMTEP\_C_{R,P}$, $CMTEP\_S_{R,P}$ and $CMTEP\_M_{R,P}$.

The $CMTEP\_C_{R,P}$ is designed to explore highly discriminative information from the center pixel. It is defined as:

$$CMTEP\_C_{R,P} = MTCP_{R,P}. \tag{15}$$

The $CMTEP\_S_{R,P}$ is equal to the traditional LBP, which can be calculated by:

$$CMTEP\_S_{R,P} = \sum_{p=0}^{P-1} s\left(g_p - g_c\right)2^p. \tag{16}$$

Like $CLBP\_M$ (see eq. (5)), the $CMTEP\_M_{R,P}$ is proposed to represent local difference magnitude information. C LBP_M uses the mean of m_p from the whole image to encode the local difference magnitude information. For an image, it is unreasonable to use a fixed threshold to quantize all pixels. Different from CLBP_M, we utilize the multi-scale hierarchical threshold (Xu *et al.*, 2020a) to $thre_{N,m_p}$ encode the local neighborhood difference, which provide a more effective local thresholding strategy. The $CMTEP\_M_{R,P}$ is defined as:

$$CMTEP\_M_{R,P} = \sum_{p=0}^{P-1} t\left(m_p, thre_{N,m_p}\right)2^p, \tag{17}$$

$$thre_{N,m_p} = \frac{1}{N}\sum_{k=1}^{N} lm\left(m_p\right), \tag{18}$$

where m_p is the local difference magnitude, $lm\left(m_p\right)$ is the local mean of m_p with scale k on the grid partitioning . N is the number of hierarchical scales.

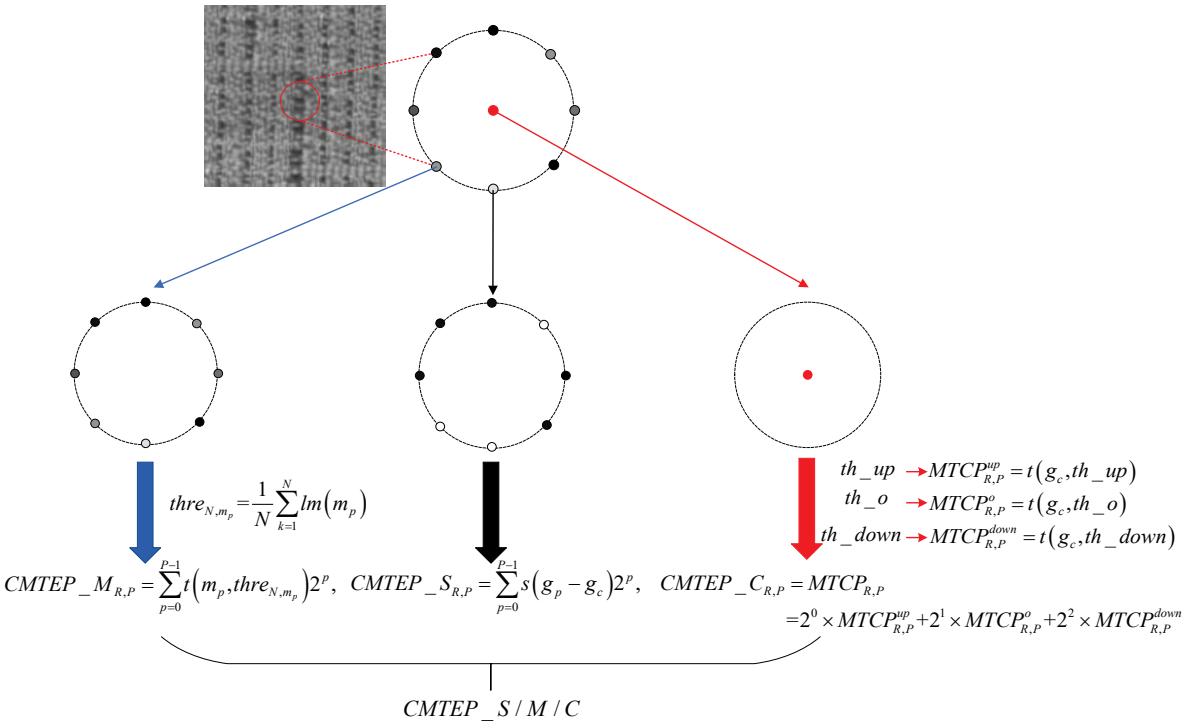

Fig. 6. *The illustration of CMTEP.*

To achieve a more comprehensive texture representation, the three sub-patterns are jointly fused, and the final texture feature is named as CMTEP_S/M/C.

RESULTS

To study the performance of the CMTEP_S/M/C descriptor for texture classification task, this paper carries out a series of comprehensive experimental evaluations on several well-known texture classification databases (such as Outex (Ojala *et al.*, 2002), UMD (Xu, 2006), and UIUC (Dana *et al.*, 1999)) with comparisons to other state-of-the-art methods.

For a fair comparison, we adopt the same classifier for each competitor, the nearest neighbor classifier. This non-parametric classifier is very suitable for feature representation and comparison purposes. In this paper, the chi-square distance is used to measure the dissimilarities between training images and sample images. The histograms of sample image and training image are described as H^S and H^T, respectively. Then the χ^2 distance can be calculated by

$$D\left(H^S, H^T\right) = \sum_{i=1}^{M} \frac{\left(H_i^S - H_i^T\right)^2}{H_i^S + H_i^T}, \tag{19}$$

where M is the number of histogram bins. And i refers to the i th bin in the corresponding histogram.

EXPERIMENTAL ANALYSIS IN OUTEX DATABASE

As one of the most widely used texture benchmarks Outex database (Ojala *et al.*, 2002) collects a wide variety of surface texture and natural scenes texture under different imaging environments. We adopt Outex_TC10 and Outex_TC12 suits to validate the rotation and illuminant invariance of our proposed CMTEP. The dimension of all texture images is 128*128. Both Outex_TC10 and Outex_TC12 contain 24 texture classes collected under three illumination conditions ("inca", "t184" and "horizon") and nine rotation angles (0°, 5°, 10^0, 15°, 30°, 45°, 60°, 75°, 90°). They all use 24*20 texture images obtained under "inca" and rotation angle 00 for training. For Outex_TC10, 24*20*8 texture samples captured under other 8 rotation angles and illumination "inca" are used as testing data. In Outex_TC12_000, testing texture images are collected under all 9 rotation angles and illumination "t184". For Outex_TC12_001, all testing samples are captured under all 9 rotation angles and illumination "horizon". Details are shown in Table 1.

The proposed CMTEP descriptor comprises four different parameters, including sampling radius (R), sampling neighborhood (P) and two floating parameters (α and β). For (R, P), we adopt general parameter setting according to most references (Guo *et al.*, 2010; Zhang *et al.*, 2017; Song *et al.*, 2015; Pan *et al.*, 2017; Xu *et al.*, 2020a; 2021). The values of (R, P) for each experiment are all listed in the experimental figure or table. For α and β, we introduce a controlling factor $\gamma\left(0<\gamma<1\right)$ to adjust them: $\alpha = 1+\gamma$ and $\beta = 1-\gamma$. As shown in Fig.7, the impact of different γ values have been evaluated with Outex_TC10. For all (R, P) settings, CMTEP_S/M/C obtains the highest classification results in terms of accuracy with $\gamma = 0.2$. Hence, we set $\gamma = 0.2$ for all experiments in this paper.

Table 1. *Summary of Outex sets*, $\theta_1 = \{5°, 10°, 15°, 30°, 45°, 60°, 75°, 90°\}$, $\theta_2 = \{0°, 5°, 10°, 15°, 30°, 45°, 60°, 75°, 90°\}$.

Texture Database	Outex database		
	TC10	TC12_000	TC12_001
Texture classes	24	24	24
Image size (pixels)	128×128	128×128	128×128
Image per class	180	200	200
Training images number	480 (20×24)	480 (20×24)	480 (20×24)
Testing images number	3810 (160×24)	4320 (180×24)	4320 (180×24)
Training Description	Illumination(inca) Rotation(0^0)	Illumination(inca) Rotation(0^0)	Illumination(inca) Rotation(0^0)
Testing Description	Illumination(inca) Rotation(Θ_1)	Illumination(t148) Rotation(Θ_2)	Illumination(horizon) Rotation(Θ_2)
Experiment evaluations	Rotation invariant evaluation	Illumination and rotation invariant evaluation	Illumination and rotation invariant evaluation

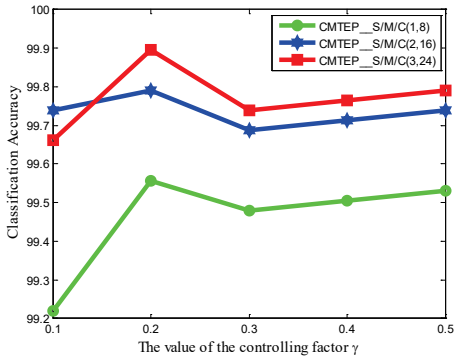

Fig. 7. *The classification results with different controlling factor values for CMTEP_S/M/C in Outex_TC10.*

To verify the improvement introduced by each of the three components of CMTEP, we conduct an ablation study in Outex_TC10. As shown in Fig.8, we present classification results used leaving one of the three components (including CMTEP_S, CMTEP_M, CMTEP_C) out at a time, and leaving out each of the three components individually. More specifically, for CMTEP_C) out at a time, and leaving out each of the three components individually. More specifically, for (R, P) = (1, 8), CMTEP_S obtains a classification accuracy of 78.91%. After introducing CMTEP_M and CMTEP_C, CMTEP_M/C and CMTEP_S/C provide better classification results of 97.84% and 98.85%, respectively. The final descriptor, CMTEP_S/M/C, reaches the highest classification accuracy of 99.56%. Hence, each component of CMTEP offers discriminative texture information for the performance improvement. Similar conclusions can be found for (R, P) = (2, 16) and (3, 24).

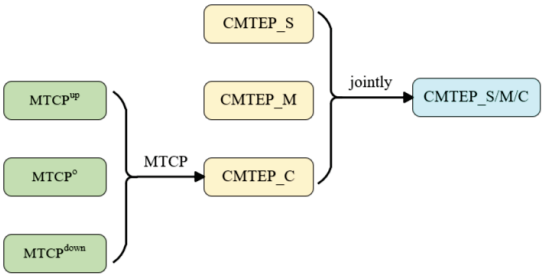

(a) The feature fusion of CMTEP_S/M/C.

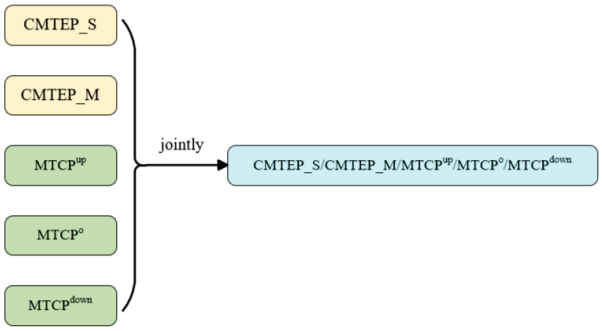

(b) The feature fusion of CMTEP_S/CMTEP_M/MTCPup/MTCPo/MTCPdown.

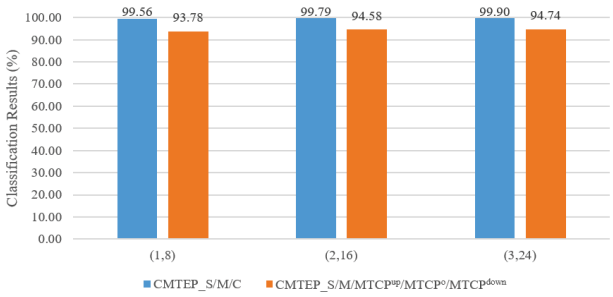

(c) Performance comparison

Fig. 9. *The comparison between CMTEP_S/M/C and CMTEP_S/CMTEP_M/MTCPup/MTCPo/MTCPdown.*

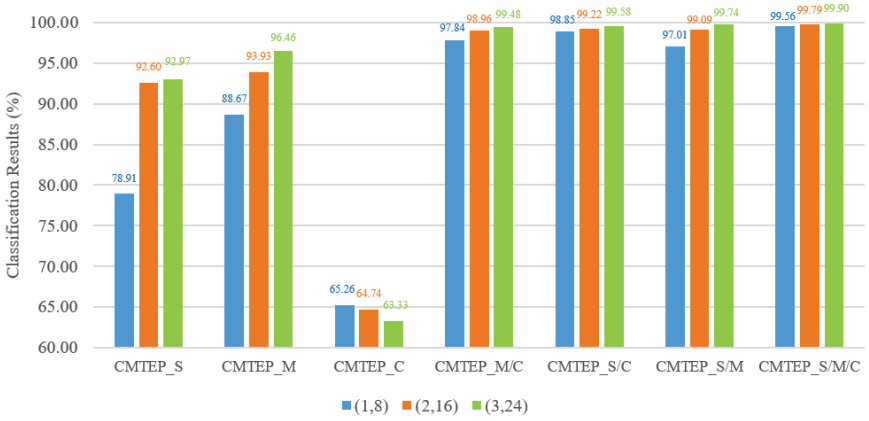

Fig. 8. *Ablation studies of CMTEP with (R, P) = (1, 8), (2, 16) and (3, 24).*

Table 2. *Classification result in terms of accuracy (%) in Outex database.*

Descriptors	(R,P)	Test sets		
		TC10	TC12_000	TC12_001
LBP (Ojala *et al.*, 2002)	(1,8)	84.81	65.46	63.68
	(2,16)	89.40	82.26	75.20
	(3,24)	**95.07**	85.04	**80.78**
BRINT (Liu *et al.*, 2014)	(1,8)	91.90	86.69	88.43
	(2,16)	96.51	93.50	94.35
	(3,24)	96.04	94.49	94.35
CLBP (Guo *et al.*, 2010)	(1,8)	96.56	90.30	92.29
	(2,16)	98.72	93.54	93.91
	(3,24)	**98.93**	**95.32**	**94.53**
AECLBP (Song *et al.*, 2015)	(1,8)	97.58	91.83	91.81
	(2,16)	98.80	95.42	94.70
	(3,24)	99.19	96.83	95.05
CDLF (Zhang *et al.*, 2017)	(1,8)	97.29	91.06	93.31
	(2,16)	99.48	94.24	95.02
	(3,24)	99.11	95.65	95.25
CLBC (Zhao *et al.*, 2012)	(1,8)	97.16	89.79	92.92
	(2,16)	98.54	93.26	**94.07**
	(3,24)	98.78	94.00	93.24
MRELBP (Li *et al.*, 2016)	(1,8)	91.17	84.95	87.01
	(3,8)	98.23	97.73	96.25
	(5,8)	93.78	89.68	89.28
CRLBP (Zhao *et al.*, 2013)	(1,8)	97.55	91.94	92.45
	(2,16)	98.59	95.88	96.41
	(3,24)	99.35	96.83	96.16
SCLBP_TC (Nguyen *et al.*, 2014)	(1,8)	98.25	92.45	94.25
	(2,16)	99.36	95.05	96.47
	(3,24)	99.45	**96.68**	98.25
$CRDP_{3D}$_2 (Wang *et al.*, 2017)	(1,8)	97.03	92.69	94.81
	(2,16)	98.33	96.41	94.95
	(3,24)	98.52	95.46	91.44
LNP (Wang *et al.*, 2015)	-	**94.97**	80.93	83.77
AGLBP (Hao *et al.*, 2017)	-	99.22	97.84	97.38
SLGP_CR_RR (Song *et al.*, 2018)	-	97.79	84.17	83.82
SALBP (Pan *et al.*, 2020)	-	99.38	96.94	96.06
DLABP (Pan *et al.*, 2017)	-	**99.04**	**95.35**	95.93
CJLBP (Wu and Sun, 2017)	-	**99.77**	**98.59**	98.68
dLBP_DMC (Hu *et al.*, 2018)	-	**99.60**	**97.96**	98.63
LGONBP (Song *et al.*, 2021)	-	**99.71**	98.59	**98.89**
EMLBP (Shakoor *et al.*, 2017)	(1,8)	91.33	85.93	88.77
	(2,16)	98.83	95.25	**95.79**
	(3,24)	**99.61**	**96.37**	95.32
FbLBP (Pan *et al.*, 2017)	(1,8)	98.85	92.66	93.82
	(2,16)	**99.64**	**95.42**	95.69
	(3,24)	99.58	94.75	**96.78**
CLEBP (Xu *et al.*, 2020a)	(1,8)	99.58	94.79	94.93
	(2,16)	99.74	**98.17**	97.62
	(3,24)		98.03	**97.92**
CLSP (Xu *et al.*, 2020b)	(1,8)	98.93	94.91	94.81
	(2,16)	99.58	98.10	96.90
	(3,24)	99.40	98.31	97.31
CMTEP_S/M/C	(1,8)	99.56	96.55	96.88
	(2,16)	99.79	98.66	**98.47**
	(3,24)	**99.90**	**99.07**	98.31

To investigate the impact of CMTEP_C for improving the performance of CMTEP, we conduct a series of experiments in TC_10. As show in Fig.9 (a) and (b), the two descriptors have same fusion strategy as shown in Guo *et al.* (2010) and two same sub-components: CMTEP_S and CMTEP_M. The difference is that CMTEP_ C is equal to MTCP, encoded by formula (14). We directly use three 1-bit MTCPup, MTCPo and MTCPdown to conduct feature fusion in CMTEP_S/CMTEP_M/MTCPup/MTCPo/MTCPdown. We can find in Fig.9(c) that CMTEP_S/M/C outperforms CMTEP_S/CMTEP_M/MTCPup/MTCPo/MTCPdown dramatically with all sampling resolutions: (R, P) = (1, 8), (2, 16) and (3, 24). The performance superiority comes from the fact that CMTEP_C efficiently alleviates the feature dimension unbalance problem by encoding three 1-bit binary patterns into a 3-bit binary code.

Table 2 illustrates the evaluation results of the CMTEP and some popular competitors on Outex_TC10 and Outex_TC12. (R, P) represents the sampling resolution. On Outex_TC10, our CMTEP achieves the best classification accuracy of 99.90% with (R, P) = (3, 24), which outperforms the LBP, LNP, and CLBP by 4.83%, 4.93%, and 0.97%, respectively. Compared with some state-of-the-art texture descriptors, CMTEP offers 0.86%, 0.13% and 0.30% improvements over the best result of DLABP, CJLBP, and dLBP_DMC. Furthermore, compared to recent texture classification methods, it also obtains an improvement of 0.19%, 0.29%, and 0.26% over LGONBP, EMLBP, and FbLBP, and slightly outperforms the best accuracy of CLEBP with (R, P) = (3, 24). The results demonstrate that the proposed CMTEP descriptor is very discriminative and powerful for the image rotation task.

For Outex_TC12, the proposed CMTEP reaches the best accuracy of 99.07% with (R, P) = (3, 24) on Outex_TC12_000, that keeps a superiority of 3.75% to CLBP. Compared to some popular texture descriptors, it outperforms DLABP, SCLBP_TC, CJLBP, and dLBP_DMC by 3.72%, 2.39%, 0.48%, and 1.11%. Moreover, our CMTEP also gains an accuracy superiority of 2.70%, 3.65%, and 0.90% to EMLBP, FbLBP, and CLEBP, respectively. For Outex_TC12_001, the best classification accuracy of CMTEP reaches 98.47% with (R, P) = (2, 16), outperforming LBP, CLBP, and CLBC by 17.69%, 3.94%, and 4.40%. Compared to some recent texture descriptors, the proposed method is higher than EMLBP, FbLBP, and CLEBP by 2.68%, 1.69%, and 0.55%, respectively. It is worth noting that our CMTEP performs very slightly worse than LGONBP in TC12_001, but outperforms it in TC10 and TC12_000. This performance superiority of CMTEP proves that our multi-threshold encoding strategy is beneficial for the classification performance.

EXPERIMENTAL ANALYSIS IN UMD DATABASE

For evaluating the performance of the CMTEP, some contrastive experiments have been carried out on UMD database (Xu, 2006). It contains 25 texture classes and each class consists of 40 texture samples obtained under different scales, viewpoints and rotations with a high resolution of 1280*960. In this section, N images (N = 20, 15, 10, and 5) are randomly chosen from each class as the training set, and the rest is used as the testing set. As the final result, we investigate the mean accuracy of the classifier over 50 time random selections. Table 3 lists the results of our CMTEP and other popular texture descriptors.

It can be found that CMTEP achieves the highest accuracy of 99.12%, 98.75%, 97.99%, and 95.23% with (R, P) = (5, 24) corresponding to the training samples 20, 15, 10, and 5, which provides an improvement of 12.87%, 14.76%, 17.52%, and 22.98% over the traditional LBP for each training samples number. Compared with the base texture descriptor CLBP, the proposed CMTEP improves the texture classification result by 5.96%, 6.14%, 7.14%, and 8.47% with (R, P) = (5, 24) for different training samples numbers. It is clear that our CMTEP provides very significant performance enhancements especially for a small training samples number.

Moreover, the CMTEP provides very competitive classification results compared to some successful binary pattern methods. More precisely, it also outperforms the best result of LTP, BRINT, MRELBP, and CRDP by 8.69%, 6.16%, 4.82%, and 7.02% with 20 training samples. In addition, the best classification accuracy of our CMTEP (99.12%) is much higher than the best accuracy of CLSP (98.49%) published in 2020. Similar findings can also be found with other numbers of training samples. The experimental results in TC12 show that the proposed CMTEP descriptor enhances the effectiveness for illumination and rotation invariance. The obtained classification performance is mainly caused by the proposed multiple threshold center pattern that adopts the multiple threshold encoding strategy in order to explore highly discriminative information from center pixels.

Table 3. *Classification result in terms of accuracy (%) in Outex database.*

Descriptors	(R,P)	The number of training images			
		20	15	10	5
LBP (Ojala *et al.*, 2002)	(1,8)	84.09	81.80	77.89	70.28
	(2,16)	84.67	82.28	7873	70.81
	(3,24)	**86.25**	**83.99**	**80.47**	**72.25**
LTP (Tan and Triggs, 2010)	(1,8)	84.24	82.48	79.14	71.71
	(2,16)	87.73	86.33	83.43	76.45
	(3,24)	89.30	87.37	84.75	77.57
	(5,24)	**90.43**	89.08	85.78	78.81
BRINT (Liu *et al.*, 2014)	(2,8)	91.87	90.92	89.38	84.91
	(3,8)	92.34	90.74	90.10	85.42
	(5,8)	**92.96**	91.92	90.32	84.63
MRELBP (Li *et al.*, 2016)	(2,8)	93.58	92.72	91.36	88.10
	(3,8)	**94.30**	93.85	92.87	89.31
	(5,8)	94.15	93.85	92.06	87.29
CRDP (Wang *et al.*, 2017)	(1,8)	91.82	90.93	89.45	85.15
	(2,16)	91.91	91.13	89.52	84.79
	(3,24)	**92.10**	91.16	89.24	84.11
	(5,24)	92.06	91.05	88.87	83.26
CLBP (Guo *et al.*, 2010)	(1,8)	92.16	91.56	90.31	86.95
	(2,16)	92.82	92.16	90.62	87.04
	(3,24)	92.87	92.14	90.48	87.55
	(5,24)	**93.16**	**92.61**	**90.85**	**86.76**
AELTP (Song *et al.*, 2015)	(1,8)	89.10	86.06	82.59	73.46
	(2,16)	91.94	91.24	86.84	80.71
	(3,24)	94.17	91.58	88.91	80.43
CLSP (Xu *et al.*, 2020b)	(3,24)	97.84	97.03	95.55	90.97
	(5,24)	**98.49**	97.24	96.39	92.00
CMTEP_S/M/C	(2,8)	99.04	98.55	97.96	95.56
	(2,16)	98.94	98.55	98.03	**95.99**
	(3,16)	99.08	98.73	97.82	95.48
	(3,24)	98.98	98.73	**98.03**	95.76
	(5,24)	**99.12**	**98.75**	**97.99**	**95.23**

EXPERIMENTAL ANALYSIS IN UIUC DATABASE

For a more comprehensive performance evaluation, this paper also carries out comparative experiments on UIUC database (Dana *et al.*, 1999). It has 25 texture classes and each one contains 40 texture images collected from different viewpoints. All images have a size of 640*480 pixels. For each class, N images (N=20, 15, 10, and 5) are randomly chosen as training data, and the rest is used as testing data. Here, this paper randomly performs this operation 50 times and reports the average of classification accuracies as the experimental results which are listed in Table 4.

As shown in Table 4, our CMTEP gets the highest classification score of 96.76%, 95.78%, 93.40%, and 87.11% with (R, P) = (5, 24) corresponding to 20, 15, 10, and 5 training samples. It significantly outperforms the base texture descriptor CLBP by 5.57%, 6.57%, 7.45% and 9.06% for different training sample numbers. Furthermore, compared to other CLBP variants with 20 training samples, CMTEP provides an improvement of 5.37%, 3.93%, and 4.58% over the best result of CLBC, CRLBP, and AECLBP. In addition, it provides a better classification score than some state-of-the-art methods. More precisely, the proposed CMTEP outperforms CDLF-AHA, FbLBP, EMCLBP, and SALBP by 2.66%, 2.59%, 3.77%, and 2.43% with 20 training samples. It also performs slightly higher than the recent CLEBP by 0.36% and outperforms the CLSP published in 2020 by 2.26%. The classification performance demonstrates that the proposed CMTEP descriptor is discriminative and powerful for the texture classification tasks in various challenging situations.

Table 4. *Classification result in terms of accuracy (%) in UIUC database.*

Descriptors	(R,P)	The number of training images			
		20	15	10	5
LBP (Ojala *et al.*, 2002)	(1,8)	54.65	52.94	47.14	39.72
	(2,16)	61.32	56.42	51.16	42.67
	(3,24)	64.05	60.05	54.25	44.59
CLBP (Guo *et al.*, 2010)	(1,8)	87.64	85.70	82.65	75.05
	(2,16)	91.04	89.42	86.29	78.57
	(3,24)	**91.19**	**89.21**	**85.95**	**78.05**
CLBC (Zhao *et al.*, 2012)	(1,8)	87.83	85.66	82.35	74.57
	(2,16)	91.04	89.66	86.63	79.48
	(3,24)	**91.39**	90.10	86.45	79.75
CRLBP (Zhao *et al.*, 2013)	(1,8)	88.08	86.62	82.97	76.01
	(2,16)	91.99	90.41	88.04	81.49
	(3,24)	**92.83**	90.55	88.02	80.54
BRINT (Liu *et al.*, 2014)	(1,8)	79.52	76.14	71.26	61.59
	(2,16)	84.14	81.57	77.06	67.96
	(3,24)	86.39	83.77	79.33	70.34
AECLBP (Song *et al.*, 2015)	(1,8)	88.04	86.54	82.96	75.43
	(2,16)	90.68	89.18	85.17	78.13
	(3,24)	**92.18**	90.22	87.08	79.69
AELTP (Song *et al.*, 2015)	(1,8)	69.16	65.41	60.88	49.93
	(2,16)	78.26	75.54	70.20	61.27
	(3,24)	82.16	79.36	72.77	63.45
LQC_C(6)N(4) (Zhao *et al.*, 2016)	(1,8)	90.12	88.54	85.62	78.38
	(2,16)	92.62	90.76	87.97	81.98
	(3,24)	93.17	90.91	88.13	81.77
CDLF AHA (Zhang *et al.*, 2017)	(1,8)	90.16	88.30	85.17	78.82
	(2,16)	**94.10**	90.53	89.58	80.82
	(3,24)	93.77	92.83	88.80	82.11
FbLBP (Pan *et al.*, 2017)	(1,8)	92.04	90.27	87.80	80.10
	(2,16)	94.14	92.73	89.79	82.43
	(3,24)	**94.17**	92.58	89.51	81.79
DLABP (Pan *et al.*, 2017)	(P=8)	92.34	90.42	87.64	80.45
EMCLBP (Shakoor *et al.*, 2017)	(1,8)	87.92	84.37	83.30	75.30
	(2,16)	92.19	90.59	87.72	80.46
	(3,24)	**92.99**	91.29	88.11	80.47
SALBP (Pan *et al.*, 2020)	(R=2)	91.20	89.69	86.83	80.05
	(R=3)	92.27	90.83	88.07	81.68
	(R=4)	93.74	92.16	89.46	82.39
	(R=5)	**94.33**	92.83	89.94	83.42
CLEBP (Xu *et al.*, 2020a)	(1,8)	93.54	91.65	89.01	82.29
	(2,16)	95.54	93.98	91.35	84.75
	(3,24)	**96.40**	94.96	92.67	86.36
CLSP (Xu *et al.*, 2020b)	(3,24)	**94.50**	92.82	90.01	85.51
CMTEP_S/M/C	(2,8)	95.63	94.41	92.29	86.25
	(3,16)	96.58	95.56	**93.85**	**87.75**
	(5,24)	**96.76**	**95.78**	**93.40**	**87.11**

DISCUSSION

The proposed CMTEP descriptor jointly fuses local sign pattern, local magnitude pattern, and MTCP to provide comprehensive texture representation. It is worth noting that the proposed MTCP combines three 1-bit binary sub-patterns into a 3-bit pattern to provide a promising texture representation and a satisfying feature simplicity. Moreover, it relieves the serious unbalance of expressive power between the traditional center based sub-pattern and local neighborhood based sub-patterns.

To verify the good performance of the proposed CMTEP, we compare the classification results in three public texture databases as shown in Fig. 10. Here, LBP, CLBP, BRINT, CLSP and the proposed CMTEP are

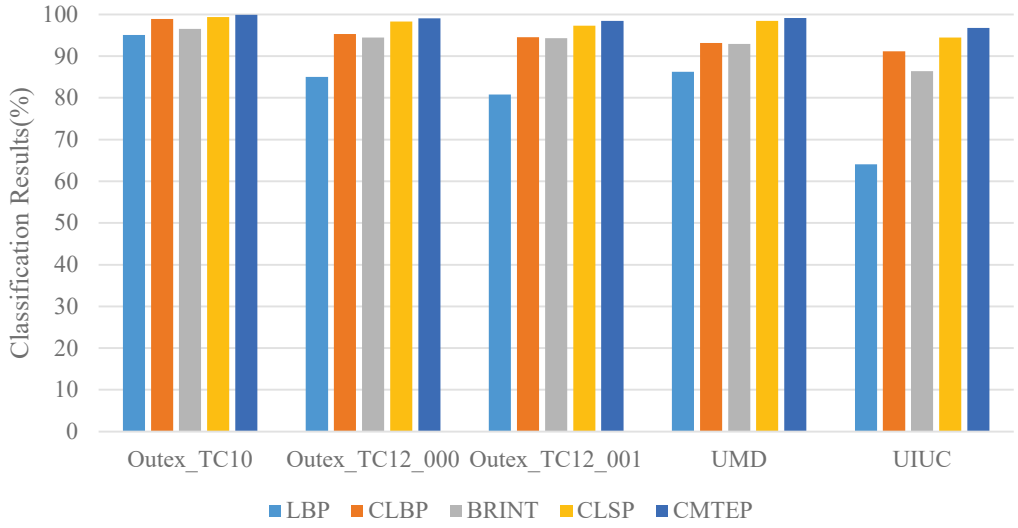

Fig. 10. *Performance comparison in Outex, UMD and UIUC databases.*

adopted for comparison experiments. It is worth noting that we pick the best result for each descriptor for every database independently. Overall, the classification results of CMTEP in the three databases are much better than the classical LBP descriptor. Moreover, the proposed CMTEP also outperforms representative successful texture classification methods, such as CLBP and BRINT. Significantly, our CMTEP achieves better results than the state-of-the-art CLSP. The performance superiority comes from the fact that the proposed MTCP efficiently alleviates the feature dimension unbalance problem by encoding three 1-bit binary patterns into a 3-bit binary code. Therefore, the CMTEP is an efficient and informative descriptor for texture classification tasks.

CONCLUSION

In order to relieve the serious unbalance of expressive power between the traditional center based sub-pattern and local neighborhood based sub-patterns, this paper presents a multiple threshold center pattern (MTCP) to extract more discriminative texture information by encoding the center pixel. It utilizes a multiple threshold encoding strategy to encode the center pixel and generate three 1-bit binary patterns. Then the 3-bit MTCP is achieved by combining these three 1-bit patterns in a compact fusion way, that provides a promising texture representation and a satisfying feature simplicity. To offer a more comprehensive texture representation, this paper proposes a completed multiple threshold encoding pattern (CMTEP) by fusing the MTCP, local sign pattern, and local magnitude pattern. The superiority of our proposed CMTEP is verified on three popular texture classification databases. In future work, we will explore a self-driven multiple threshold selection strategy for MTCP to improve the discriminative power of the texture classification system. In addition, we will try to use our proposed CMTEP to solve some problems in application areas, such as fabric identification in textile industry, high similarity plant recognition in ecology, and micro-expression recognition in intelligence system.

ACKNOWLEDGMENTS

The paper is funded by the National Key Research and Development Program of China under Grant No. 2016YFF0102806, the National Natural Science Foundation of China under Grant No. 51809056, the Natural Science Foundation of Heilongjiang Province, China, under Grant No. F2017004.

REFERENCES

Armi L, Fekri-Ershad S (2019). Texture image Classification based on improved local Quinary patterns. Multimed Tools Appl 78(14): 18995-9018.

Chakraborty S, Singh SK, Chakraborty P (2017a). Local directional gradient pattern: a local descriptor for face recognition. Multimed Tools Appl 76:1201-16.

Chakraborty S, Singh SK, Chakraborty P (2017b). Local quadruple pattern: A novel descriptor for facial image recognition and retrieval. Comput Electr Eng 62: 92-104.

Chakraborty S, Singh SK, Chakraborty P (2018). Local Gradient Hexa Pattern: A Descriptor for Face Recognition and Retrieval. IEEE T Circ Syst Vid 28(1):171-80.

Dana KJ, Van Ginneken B, Nayar SK, Koenderink JJ (1999). Reflectance and texture of real-world surfaces. ACM T Graphic 18(1): 1-34.

Dimitropoulos K, Barmpoutis P, Grammalidis N (2017). Higher Order Linear Dynamical Systems for Smoke Detection in Video Surveillance Applications. IEEE T Circ Syst Vid 27(5): 1143-54.

Fei L, Zhang B, Xu Y, Huang D, Jia W, Wen J (2020). Local Discriminant Direction Binary Pattern for Palmprint Representation and Recognition. IEEE T Circ Syst Vid 30(2): 468-81.

Guo Z, Zhang L, Zhang D (2010). A Completed Modeling of Local Binary Pattern Operator for Texture Classification. IEEE T Image Process 19(6): 1657-63.

Hao Y, Li S, Mo H, Li H (2017). Affine-Gradient Based Local Binary Pattern Descriptor for Texture Classification. Proceedings Of ICIG 2017, 10666. Springer, Cham, 199-210.

Hu R, Li X, Guo Z (2018). Decorrelated local binary patterns for efficient texture classification. Multimed Tools Appl 77: 6863-82.

Lee JY, Lin JL, Chen YW, Chang YL, Kovliga I, Fartukov A, Lei SM (2015). Depth-Based Texture Coding in AVC-Compatible 3D Video Cod-ing. IEEE T Circ Syst Vid 25(8): 1347-61.

Li L, Lao S, Fieguth PW, Guo Y, Wang X, Pietikäinen M (2016). Median Robust Extended Local Binary Pattern for Texture Clas-sification. IEEE T Image Process 25(3): 1368-81.

Li Y, Xu X, Li B, Ye F, Dong Q. (2018). Circular regional mean completed local binary pattern for texture classifica-tion. J Electron Imaging 27(4).

Liu L, Long Y, Fieguth PW, Lao S, Zhao G (2014). BRINT: Binary Rotation Invariant and Noise Tolerant Texture Classi-fication. IEEE T Image Process 23(7): 3071-84

Murala S, Maheshwari RP, Balasubramanian R (2012). Local Tetra Patterns: A New Feature Descriptor for Content-Based Image Retrieval. IEEE T Image Process 21(5): 2874-86.

Nanni L, Lumini R, Brahnam R (2010). Local binary patterns variants as texture descriptors for medical image analysis. ARTIF Intell Med 49(2): 117-25.

Nguyen, V. D., Nguyen, D. D., Nguyen, T. T., Dinh, V. Q., & Jeon, J. W. (2014). Sup-port Local Pattern and its Application to Disparity Im-provement and Texture Classification. IEEE T Circ Syst Vid 24(2): 263-76.

Nie R, Cao J, Zhou D, Qian W (2021). Multi-Source Information Exchange Encoding with PCNN for Medical Image Fusion. IEEE T Circ Syst Vid 31(3): 986-1000.

Ojala T, Maenpaa T, Pietikainen M, Viertola J, Kyllonen J, Huovinen S (2002). Outex - new framework for empirical evaluation of texture analysis algorithms. Proceedings Of ICPR 2002, Quebec City, QC, Canada, 701-6.

Ojala T, Pietikainen M, Maenpaa T (2002). Multiresolution gray-scale and rotation invariant texture classification with local binary patterns. IEEE T Pattern Anal 24(7): 971-87.

Pan Z, Li Z, Fan H, Wu X (2017). Feature based local binary pattern for rotation invariant texture classification. Expert Syst Appl 88: 238-48.

Pan Z, Wu X, Li Z, Zhou Z (2017). Local Adaptive Binary Patterns Using Diamond Sampling Structure for Texture Classification. IEEE Signal Proc Let 24(6): 828-32.

Pan Z, Wu X, Li Z (2020). Scale-adaptive local binary pattern for texture classification. Multimed Tools Appl 79: 5477-500.

Shakoor MH, Boostani R (2017). Extended Mapping Local Binary Pattern Operator for Texture Classification. Int J Pattern Recogn 31(6): 1-22.

Song K, Yan Y, Zhao Y, Liu C (2015). Adjacent evaluation of local binary pattern for texture classification. J Vis Commun Image R 33: 323-39.

Song T, Feng J, Luo L, Gao C, Li H (2021). Robust Texture Description Using Local Grouped Order Pattern and Non-Local Binary Pattern. IEEE T Circ Syst Vid 31(1):189-202.

Song T, Li H, Meng F, Wu Q, Cai J (2018). LETRIST: Locally Encoded Transform Feature Histogram for Rotation-Invariant Texture Classification. IEEE T Circ Syst Vid 28(7): 1565-79.

Song T, Xin L, Gao C, Zhang G, Zhang T (2018). Gray-scale-Inversion and Rotation Invariant Texture Description Using Sorted Local Gradient Pattern. IEEE Signal Proc Let 25(5): 625-9.

Sotoodeh M, Moosavi MR, Boostani R (2019). A Novel Adaptive LBP-Based Descriptor for Color Image Retrieval. Expert Syst Appl 127: 342-52.

Tan X, Triggs B (2010). Enhanced Local Texture Feature Sets for Face Recognition Under Difficult Lighting Conditions. IEEE T Image Process 19(6):1635-50.

Taha B, Hayat M, Berretti S, Hatzinakos D, Werghi N (2020). Learned 3D Shape Representations Using Fused Geometrically Augmented Images: Application to Facial Expression and Action Unit Detection. IEEE T Circ Syst Vid 30(9): 2900-16.

Wang K, Bichot CE, Li Y, Li B (2017). Local binary circumferential and radial derivative pattern for texture classification. Pattern Recogn 67: 213-29.

Wang S, Wu Q, He X, Yang J, Wang Y (2015). Local N - Ary Pattern and Its Extension for Texture Classification. IEEE T Circ Syst VID 25(9): 1495-506.

Wei L, Dai HY (2016). Real-time Road Congestion Detection Based on Image Texture Analysis. Procedia Engineer 137: 196-201.

Wu X, Sun J (2017). Joint-scale LBP: a new feature descriptor for texture classification. Visual Comput 33:317-29.

Xu H (2006). A Projective Invariant for Textures. Proceedings of CVPR 2006, New York, NY, USA, 932-9.

Xu X, Li Y, Wu Q (2020a). A Multiscale Hierarchical Threshold-Based Completed Local Entropy Binary Pattern for Texture Classification. Cogn Comput 12(1): 224-37.

Xu X, Li Y, Wu Q (2020b). A completed local shrinkage pattern for texture classification. Appl Soft Comput 97: 106830.

Xu X, Li Y, Wu Q (2021). A compact multi-pattern encoding descriptor for texture classification. Digit Signal Process 114(2): 103081.

Zhang Z, Liu S, Mei X, Xiao B, Zheng L (2017). Learning completed discriminative local features for texture classification. Pattern Recogn 67: 263-75.

Zhao Y, Huang DS, Jia W (2012). Completed Local Binary Count for Rotation Invariant Texture Classification. IEEE T Image Process 21(10): 4492-7.

Zhao Y, Wang RG, Wang WM, Gao W (2016). Local Quan-tization Code Histogram for Texture Classification. Neurocomputing 207(26): 354-64.

Zhao Y, Jia W, Hu RX, Min H (2013). Completed robust lo-cal binary pattern for texture classification. Neurocom-puting 106(15): 68-76.